Published August 8, 2019

Original Research

Core Ideas

- Our aim was to test whether mucilage promotes diffusion of nutrients in dry soil.
- Mucilage favors transport of nutrients in drying soil and their uptake by plant.
- Mucilage increases the soil moisture in the rhizosphere as soil dries.
- Mucilage maintains the connectivity of liquid phase in the rhizosphere as soil dries.

Mucilage Facilitates Nutrient Diffusion in the Drying Rhizosphere

Mohsen Zarebanadkouki,* Theresa Fink, Pascal Benard, and Callum C. Banfield

Despite detailed investigations of its distinct biochemical properties and their effects on the availability of nutrients for plants, the biophysical aspects of the rhizosphere, particularly the effect of mucilage on the transport of water and nutrients, are poorly understood. The aim of this study was to investigate the effect of mucilage on the diffusion of nutrients and consequently their transport through the rhizosphere into the plant roots. Phosphor imaging technique determined the temporospatial distribution of ^{137}Cs in a model rhizosphere (a sandy soil mixed with chia seed (*Salvia hispanica* L) mucilage. The observed profiles of activities were used to estimate the diffusion coefficient of K in soils. A diffusion–convection equation was numerically solved to predict the transport of K and its uptake by a single plant root in drying soil. The results suggest that mucilage (i) keeps the rhizosphere wet and (ii) maintains the connectivity of the liquid phase in drying soil. In these ways, mucilage moderates the drop in diffusive transport. The modeling results showed that the presence of mucilage in the rhizosphere (i) prevents depletion of nutrients in soils with a low nutrient concentration in the soil solution and (ii) delays the risk of nutrient and/or salt accumulation in the vicinity of the root in soils with a high concentration nutrient and/or salt the soil solution. In conclusion, mucilage appears to mitigate the risk of nutrient deficiency and salinity stress as it enhances the diffusive transport in drying soil. In this way, mucilage may favor the transport of nutrients within the rhizosphere and their uptake by plant roots in drying soil.

M. Zarebanadkouki and P. Benard, Soil Physics Group, Univ. of Bayreuth, 95440 Bayreuth, Germany; T. Fink, Institute for Soil Science of Temperate Ecosystems, Univ. of Göttingen, 37073 Göttingen, Germany; C.C. Banfield, Biogeochemistry of Agricultural Ecosystems, Univ. of Goettingen, 37073 Göttingen, Germany. *Corresponding author (Mohsen.zarebanadkouki@uni-bayreuth.de).

Received 28 Feb. 2019.
Accepted 18 May 2019.
Supplemental material online.

Citation: Zarebanadkouki, M., T. Fink, P. Benard, and C.C. Banefield. 2019. Mucilage facilitates nutrient diffusion in the drying rhizosphere. Vadose Zone J. 18:190021. doi:10.2136/vzj2019.02.0021

The ability of plant roots to extract nutrients from soil depends largely on nutrient availability in their vicinity, *the rhizosphere*. The rhizosphere is a biological hotspot, defined as the region of soil affected by plant root growth and exudation. The symbiosis of plants and microorganisms in the rhizosphere has been extensively studied and is known to play an important role in nutrient cycling (Walker, 2003; Hinsinger et al., 2009; Kuzyakov, 2010). By alteration of the biochemical properties in this region, plant roots, directly and indirectly, increase the bioavailability of nutrients through mobilization, transformation, and acquisition of nutrients from the soil. Root-induced modifications are triggered by the release of substantial amounts of photosynthates like organic acids, chelating agents, sugars, amino acids, and enzymes (Walker et al., 2003; Jones et al., 2009; Oburger and Jones, 2018). The transport of nutrients within the soil is another key factor controlling the bioavailability of nutrients. It is primarily controlled by the physical properties of the soil affecting both mass flow and diffusion. In contrast with the biochemistry, the effects of plant-induced physical alterations of the rhizosphere have barely been explored.

The soil water content plays a critical role in restricting mass flow and diffusion of nutrients within the soil pore spaces. The relative importance of mass flow is determined by the rate of root water uptake and the concentration of nutrients in the soil solution. As the soil dries, its hydraulic conductivity drops by several orders of magnitude, restricting the flow of water and nutrients. When mass flow does not match the plant's demand, the concentration of nutrients in the vicinity of the roots decreases (Seiffert et al., 1995). The developed gradient in concentration is partly attenuated by diffusion of nutrients toward this depletion zone at the root surface. As soil water content decreases, (i) the cross-sectional area of the liquid phase decreases, and (ii) the average diffusion path of nutrients to

reach the root surface increases (tortuosity). Both processes limit the diffusion of nutrients in drying soil (Moldrup et al., 2001; Chou et al., 2012). Additionally, a reduction of soil water content reduces the availability of buffered ions by shifting the equilibrium between the concentration of nutrients in the liquid and the solid phase toward the solid phase (Darrah, 1993). Soil drying also influences the availability of critical nutrients (e. g. N and P) by limiting microbial activity (Moyano et al., 2013).

Plants may alter their surrounding soil environment to buffer unpredictable fluctuations in water content and related negative effects on soil hydraulic properties. The physical properties of the rhizosphere were shown to be altered by mucilage, a highly polymeric gel released at the root tip. Mucilage primarily consists of polysaccharides, lipids, and root border cells (Oades, 1978). Mucilage enhances the rhizosheath formation and therefore may reduce the risk of gap formation between root and soil under drying conditions. Mucilage can absorb substantial quantities of water and therefore increases the water-holding capacity of the rhizosphere (McCully and Boyer, 1997; Kroener et al., 2014). In this way, the rhizosphere remains moist and could facilitate root water uptake by preventing a sharp drop in hydraulic conductivity of soil close to the root surface. Besides its intrinsic hygroscopic nature, mucilage lowers the surface tension at the gas–liquid interface and increases the viscosity of the soil solution (Read and Gregory, 1997). The interplay between water absorption, surface tension, and viscosity was shown to alter the spatial configuration of the liquid phase in drying soil (Carminati et al., 2017; Benard et al., 2018, 2019).

The motivation of this study was to test whether mucilage promotes the diffusion of nutrients in dry soil. This study was inspired by the conceptual model proposed by Benard et al. (2018), which is briefly discussed in the section below. Note, that the focus of the current work lies on the physical aspects of root–soil interactions, and the discussion of chemical and biological aspects is not part of it. Here, a phosphor imaging technique was used to visualize the spatial distribution of K by its proxy ^{137}Cs (mixed with ^{133}Cs) within a model rhizosphere soil. To mimic the rhizosphere soil, a washed sandy soil (with no organic matter) was mixed with different mucilage contents extracted from chia seeds (*Salvia hispanica* L). Subsequently, a concentration gradient of Cs was induced, and the resulting diffusion was monitored by ^{137}Cs phosphor imaging under different soil water and mucilage contents. The monitored profiles of ^{137}Cs were inversely simulated to estimate the diffusion coefficient of soils as a function of mucilage and soil water content. As a first estimation, the effect of mucilage on the concentration of K in the soil and its uptake by plants were evaluated by solving a simple diffusion–convection model. The model included the uptake of K into a single root and was parameterized based on the data of K uptake by Seiffert et al. (1995). The hydraulic and diffusive properties of the soil were parameterized based on our measurements, and then different scenarios varying in terms of mucilage presence, K concentration in the soil solution, and root water uptake rate were tested. For simplicity, an identical effect of mucilage on the diffusion of K and ^{137}Cs in the soil was assumed. Mucilage extracted from chia seeds was used as a root mucilage analog, as it can be extracted in sufficient quantities required to test our concepts. Chia seed mucilage was shown to differ from maize (*Zea mays* L.) and barley (*Hordeum vulgare* L.) seedling mucilage. In particular, it is more viscous (Naveed et al., 2019). On the other hand, the physical properties of mucilage collected from plant seedlings were shown to be plant specific and concentration dependent, which makes it challenging to select a mucilage representative of mucilage across plant species. However, besides these variations, all mucilages showed unique intrinsic physical properties: reduction of surface tension of the soil solution, increase of viscosity, increase of the water holding capacity, and turning hydrophobic as they dry (Benard et al., 2019).

Conceptual Model: The Effect of Mucilage on Nutrient Availability in the Rhizosphere

When the soil dries, its pores are drained, and consequently, the cross-sectional area of the liquid phase is reduced while its tortuosity increases. With further soil drying, a critical water content is reached, at which the connectivity of the liquid phase drops abruptly (Lim et al., 1998; Moldrup et al., 2001). All these processes result in a reduction of hydraulic conductivity and diffusive transport as the soil dries. Taking into account these facts, the diffusion coefficients of nutrients as a function of soil moisture, $D(\theta)$, can be described as

$$D(\theta) = S_e^{\lambda} D_s \quad [1]$$

where S_e is the effective water saturation degree of soil, defined as

$$S_e = \left(\frac{\theta - \theta_{th}}{\theta_s - \theta_{th}} \right) \quad [2]$$

where D_s is the diffusion coefficients of a given nutrient in saturated soil (cm^2 s^{-1}), λ is a unitless factor describing the tortuosity of the diffusion path, including the connectivity of the liquid phase, its disconnection, and the effect of dead-end pores ($\lambda \geq 0$, where $\lambda = 0$ refers to a straight transport path with no restriction), θ is the soil water content (cm^3 cm^{-3}), θ_s is the saturated water content (cm^3 cm^{-3}), and θ_{th} is the critical water content at which the connectivity of the liquid phase is interrupted (cm^3 cm^{-3}). The term ($\theta - \theta_{th}$) can be interpreted as the effective water content available for nutrient diffusion (Moldrup et al., 2001).

Mucilage in the rhizosphere could affect diffusion of nutrients in two ways (Fig. 1): (i) mucilage increases the water-holding capacity of the rhizosphere, which results in a larger cross-sectional area of the liquid phase at a given soil water potential, or (ii) mucilage may alter the spatial configuration of the liquid phase during soil drying by preventing the capillary breakup of the liquid phase (Carminati et al., 2017; Benard et al., 2018). Root mucilages from different plant species share some fundamental properties. They increase the viscosity of the soil solution and lower the surface tension at the gas–liquid interface (Read and Gregory, 1997; Read et

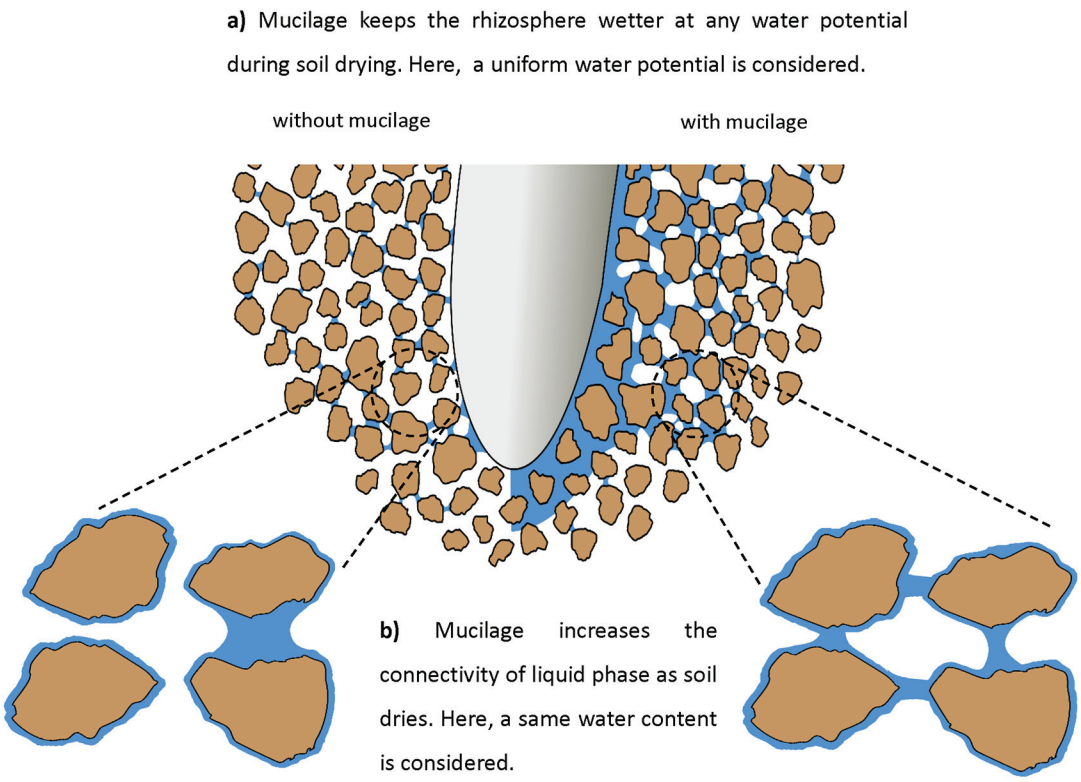

Fig. 1. Effects of mucilage on soil water content and its spatial configuration in the rhizosphere: (a) schematic sketch of a single root in soil and the effect of mucilage on soil water content of the rhizosphere—considering a uniform water potential, mucilage keeps the rhizosphere wetter than the bulk soil during soil drying; and (b) schematic sketch of mucilage effect on the spatial distribution of liquid phase between soil pores—mucilage maintains the connectivity of the liquid phase under drying conditions.

al., 1999; Naveed et al., 2017). Together with the capacity of the mucilage polymer network to absorb water (McCully and Boyer, 1997), increased viscosity and decreased surface tension were shown to help to maintain the connectivity of the soil solution during soil drying (Carminati et al., 2017; Benard et al., 2018). Under such circumstances, Eq. [1] can be further generalized to include the effect of varying mucilage contents on the diffusion coefficient of nutrients in the soil as

$$D(\theta) = S_{e^*}^{\lambda^*} D_s \quad [3]$$

where λ^* is a unitless factor describing the tortuosity of the diffusion path in soil defined as

$$\lambda^* = \lambda \exp(-\gamma C_{tot}) \quad [4]$$

where γ is a unitless fitting parameter and C_{tot} is the concentration of mucilage (g dry mucilage g^{-1} dry soil). This parameterization guarantees that mucilage reduces the tortuosity of the transport path in a soil mixed with mucilage compared with the tortuosity of its control, λ. The S_{e^*} is the effective water saturation degree of soil defined as

$$S_{e^*} = \left(\frac{\theta - \theta_{th}^*}{\theta_s - \theta_{th}^*} \right) \quad [5]$$

where θ_{th}^* is the critical water content defined as

$$\theta_{th}^* = \theta_{th} \exp(-\tau C_{tot}) \quad [6]$$

where τ is a unitless fitting parameter. This parameterization guarantees that mucilage keeps the connectivity of soil at a drier range.

Materials and Methods

Modeled Rhizosphere Soil Preparation

The effect of the rhizosphere on the diffusion of ^{137}Cs in the soil at varying water contents was studied in a model rhizosphere soil. The model rhizosphere soil was composed of washed quartz sand from a sandpit located near Duingen, Germany, with no organic matter and sieved to the particle size of 30 to 125 μm mixed with mucilage extracted from chia seeds. Chia seed mucilage was extracted as follows (Benard et al., 2017): chia seeds were mixed with water (w/w, 1:10) and stirred for 2 h. Then, the mixture was passed through two sieves with mesh sizes of 0.5 and 0.2 mm, respectively, by applying a suction of −800 hPa. The concentration of the extracted mucilage (g dry weight g^{-1} wet weight) was determined by comparing the mucilage solution's dry weight to its initial wet weight. The model rhizosphere was prepared by mixing the extracted mucilage with soil at a content of 2.5 mg g^{-1} (g dry mucilage g^{-1} dry soil). This concentration was chosen based on the results of a pre-test where the effect of varying mucilage contents of 0.5, 1, 2.5, 4, 8 mg g^{-1} dry soil on water-holding capacity

of soil at matric potentials of −60 and −100 cm was quantified (see the section below). We selected the lowest mucilage content, which increased water holding capacity of our sandy soil. It should be noted that the mucilage content in the rhizosphere varies as a function of distance from the root surface and was estimated to be 1 mg g^{-1} soil (average for a distance of 1.5 mm from the root surface; Carminati and Vetterlein, 2013). A mucilage content of 2.5 mg g^{-1} soil in this study is taken as the upper expected limit of the expected mucilage content in the immediate vicinity of the root in the rhizosphere. Additionally, the effect of mucilage on hydraulic properties of the soil will depend strongly on the particle size and plants may adapt the mucilage content in the rhizosphere depending on the soil type and growth condition (Holz et al., 2018).

Measurement of the Soil Retention Curve

The retention curves of soils with and without mucilage were measured using a combination of the hanging column method for water potentials of −3, −10, −60, and −100 cm and the pressure plate method for water potentials of −300 −700, and −1500 cm. The soil was mixed with water and mucilage at a content of 2.5 mg g^{-1} (g dry mucilage g^{-1} dry soil) and was packed into containers of 6-cm i.d. and 2-cm height while the water content of both soils was ~0.25 cm^3 cm^{-3}. The samples were filled at a given bulk density of 1.56 g cm^{-3}. Then, the samples were saturated with water for 48 h by the capillary rise method from the bottom to minimize air entrapment. Samples were subject to decreasing water potentials and allowed to equilibrate. Equilibrium was assumed to be reached when no water flowed out of the samples for at least two successive days. When equilibrium reached, the samples were weighed, and the water content was gravimetrically determined (Kroener et al., 2018). All measurements were replicated three times. The water retention curve of soil without mucilage was parameterized according to the van Genuchten equation as

$$\theta(h_m) = \theta_r + \frac{\theta_s - \theta_r}{\left[1 + \left(\alpha|h_m|\right)^n\right]^{1-1/n}} \quad [7]$$

where $\theta(h_m)$ is volumetric water content (cm^3 cm^{-3}) at any given matric potential of h_m (cm), θ_s and θ_r are saturated and residual water content (cm^3 cm^{-3}), α (cm^{-1}) and n (dimensionless) are empirical coefficients.

The retention curve of soil treated with mucilage was parameterized according to the model of Kroener et al. (2014). The model assumes that the polymeric mucilage network induces an absorptive potential that lowers the soil water potential. This absorptive potential is similar to an osmotic potential and depends on the concentration of mucilage in the liquid phase. In the presence of mucilage, the soil water potential is the sum of the matric potential and the absorptive potential

$$h = h_m(\theta) + h_a(\theta) \quad [8]$$

where h is soil water potential (cm), $h_m(\theta)$ is the matric potential of soil at any given water content (cm), and $h_a(\theta)$ is the absorptive potential induced by the presence of mucilage in the soil (cm). The relation between water potential induced by mucilage and its concentration in the liquid phase is described as

$$h_a = \omega_1\left[C_m(\theta) - C_m(\theta_s)\right]^{\beta_1} + \omega_2\left[C_m - C_{m,sat}\right]^{\beta_2} \quad [9]$$

where $C_m(\theta)$ is the mucilage content in the liquid phase at any given water content, θ (mg cm^{-3}), $C_m(\theta) = C_{tot}\rho_b/\theta$, C_{tot} is the mucilage content (mg dry mucilage g^{-1} dry soil), ρ_b denotes the bulk density of soil (g cm^{-3}), $C_m(\theta)$ denotes the mucilage content in the liquid phase when soil is saturated (mg cm^{-3}), and ω_1, β_1, ω_2, and β_2 are fitting parameters (dimensionless). The soil water content at any given water potential can then be estimated from the retention curve of soil without mucilage using Eq. [7] and taking into account that the soil water potential will be higher (more negative) in the presence of mucilage:

$$\theta(h) = \theta(h_m + h_a) \quad [10]$$

Note that in soil without mucilage, $h = h_m$.

Measurement of Saturated Hydraulic Conductivity

The effect of varying contents of mucilage extracted from chia seeds on the saturated hydraulic conductivity of soil was measured using a constant pressure head method (Eijkelkamp Soil & Water). Mucilage was mixed with soil at varying contents of 0, 0.5, 1, 2, and 5 mg g^{-1}. Cylinders of 2-cm i.d. were filled with 10 g of mucilage–soil mixture and compacted to a bulk density of 1.56 g cm^{-3}. The soil columns were saturated with water for a period of 48 h by capillary rise, and subsequently a constant water level difference of 2 cm was established between the top and the bottom of the samples, and water outflow was determined. This information (outflow [cm^3 s^{-1}], the geometry of soil, and established pressure gradient [cm]) was used to calculate the saturated hydraulic conductivity of the soil (K_s, cm s^{-1}) based on Darcy's equation (Kroener et al., 2018). The van Genuchten–Mualem equation was used to parameterize the unsaturated hydraulic conductivity of soil:

$$K(\theta) = K_s\Theta^{\lambda}\left[1 - \left(1 - \Theta^{1/m}\right)^m\right]^2 \quad [11]$$

where $K(\theta)$ is the hydraulic conductivity of the soil as a function of soil water content (cm s^{-1}), λ is a unitless fitting parameter describing the tortuosity of the flow path, and $m = 1 - 1/n$. It was assumed that λ will be equal to the one obtained from diffusion measurement. Note that here Θ is defined as $\Theta = (\theta - \theta_r)/(\theta_s - \theta_r)$ where θ_r is the residual water content. According to the model proposed by Kroener et al. (2014), Eq. [11] was further generalized to also include the effect of varying mucilage contents on hydraulic conductivity of soil, $K^*(\theta)$:

$$K^*(\theta) = \frac{\mu_w}{\mu_m}K_s\Theta^{\lambda^*}\left[1 - \left(1 - \Theta^{1/m}\right)^m\right]^2 \quad [12]$$

where μ_w is the viscosity of water (μ_w = 1 mPa s^{-1}) and λ^* is assumed to be equal to that obtained from diffusion measurement.

Here, the presence of mucilage is assumed to have two contrasting effects on the $K^*(\theta)$. Due to increasing the viscosity of the liquid phase it reduces the $K^*(\theta)$ but as soil dries it avoids big drop in $K^*(\theta)$ by maintaining the connectivity *f* liquid phase (Benard et al., 2019). With increasing mucilage concentration in the liquid phase, the viscosity of the liquid phase increases. The relation proposed by Kroener et al. (2014) was used to describe viscosity as a function of mucilage content:

$$\mu_m(c) = \mu_w \max\begin{cases} \left(C_{tot}/C_0\right)^{d_0} + 1 \\ \left(C_{tot}/C_0\right)^{d_1} \end{cases} \quad [13]$$

where C_0, C_1, d_0, and d_1 are fitting parameters (dimensionless) that were determined by fitting Eq. [12] to the measured data of saturated hydraulic conductivities of soil at different mucilage contents.

Determination of Diffusion Coefficients

Diffusion experiments were performed in aluminum containers of a size of 5 by 1.8 by 0.8 cm (length by width by height). The soil was filled into the containers as follows: the model rhizosphere soil and its control without mucilage were subdivided into two groups. Soil of one group was adjusted to water contents of either 0.30, 0.20, or 0.13 $cm^3\ cm^{-3}$ with bidistilled water, whereas the soil of the second group was adjusted to the same water contents with three radiotracer solutions containing 10 mM ^{133}CsCl and ^{137}Cs at activity concentrations from 50 to 100 kBq mL^{-1} (POLATOM). Varying activity concentrations were applied so that the total activity in each aluminum container was in a similar range to ensure comparable intensities on the storage phosphor screens (Banfield et al., 2017). The activities of all ^{137}Cs solutions were determined by the automatic gamma counter (17.5% efficiency, HiDex). Based on the measured ^{137}Cs activities and the concentration of the ^{133}CsCl solution, a conversion factor of ~2.83 was obtained to convert kilobecquerels of ^{137}Cs to the total amount of Cs (mg) in the stock solution.

After adjusting the mucilage content and soil water contents, the soils were allowed to equilibrate for 24 h. Then, the first half (2.5 cm) of each container was filled with soil (control or model rhizosphere soil) that was rewetted with the radiotracer solution (as described above). The second half of each container was filled with the soil of identical mucilage and water content but rewetted with bidistilled water. During filling, the first compartment of each container with soil a cubic block of 2.5 by 1.8 by 0.8 cm was placed in the second compartment to ensure a sharp border between both compartments. Each compartment was filled with the soil of a bulk density of 1.55 g cm^{-3} and then covered with a 12-μm Hostaphan film (Mitsubishi Polyester Film) to prevent water loss during the measurement. To facilitate the imaging procedure, 15 containers were fixed on a large plastic plate and all were kept at 21°C. All treatments were replicated five times.

Phosphor imaging was used to visualize the local distribution of ^{137}Cs five times during the experiment (i.e., 3, 17, 40, 64, and 159 h after filling the containers). Storage phosphor screens (BAS-MS 2040; 20 by 40 cm; Fujifilm Europe) were placed on the Hostaphan film for 3 h in the dark. The imaging system Typhoon FLA 9500 (GE Healthcare) was used to read the screens at a resolution of 50 μm.

The β^- radiation from the decay of ^{137}Cs was stored in 16-bit digital images. All images were processed in MATLAB (The MathWorks, 2017) to quantify the spatial distribution of Cs within the sample at varying times (Cs diffusion). Images were normalized for the background noise as follows: a blank region of each image, where the screen was not in contact with soil, was selected as a reference. The intensity in this region was averaged (referred to as ref). Then, all images were normalized by the ratio between the average intensity obtained from the reference at time *t* (any time after the labeling experiment started) and its value at the first imaging, t_1, as

$$\text{img} = 1 - \text{img}\frac{\text{ref}(t_1)}{\text{ref}(t)} \quad [14]$$

The images from different time points did not overlap pixel by pixel. The images were aligned by defining one image as the reference and applying a rigid transformation to the other. For this purpose, intensity-based image registration was used. Thanks to the high contrast between the soil containers and the surrounding background, a mask showing the position of each container could be prepared by applying a thresholding method. To do so, a threshold was applied to the images obtained at the end of the experiment when ^{137}Cs had diffused throughout the soil. This mask was used to calculate the captured intensities across the soil samples at varying times. For simplicity and since the soil was uniform, the profiles of intensities were averaged along the width of each soil sample.

The image intensity (gray value) is proportional to the ^{137}Cs activity in the soil; thus, image data can be converted to activity data. This proportionality was determined by imaging of soils with added specific activities of ^{137}Cs. A sample of 0.4 g dry soil was adjusted to a water content of 0.20 $cm^3\ cm^{-3}$ by 80 μL radiotracer solution containing activities ranging from 0 to 125 kBq mL^{-1}. The soil was homogenized and transferred to a 96-well microtiter plate (U-shaped wells, 6.94-mm diam., 11.65-mm depth; Brandplates), and a smooth soil surface was prepared. Then, the same imaging and processing procedures were applied. The intensities were related to ^{137}Cs activities. A linear regression function was fitted between intensity and ^{137}Cs activity data. Using this function, the profiles of intensities were converted to ^{137}Cs activities. In the next step, the activity of ^{137}Cs was converted to the concentration of Cs using the calculated conversion factor (2.83 mg Cs kBq^{-1}).

Measurement of the Adsorption Isotherm

The images show total radionuclide concentration within the soil. Cesium like any other cation in the soil is partitioned between liquid and solid phases (i.e., becomes adsorbed). However, to describe its diffusion within the soil, its concentration in the liquid

phase is needed. The adsorption isotherm, K_d (mL g^{-1}), describes the relation between the adsorption of cations (mg g^{-1}) and their concentration in the liquid phase (mg mL^{-1}). The adsorption isotherm of Cs in both soils with and without mucilage was determined as follows: in 50-mL 0.01 M HCl prewashed centrifugation tubes, 15 g of each soil type was equilibrated with 30 mL of CsCl at five concentrations ranging from 0.05 to 0.001 M. The solutions were labeled with ^{137}Cs activities ranging from 20 to 1000 Bq mL^{-1}, which were determined by the HiDex automatic gamma counter. The solutions were added to the soil, shaken for 10 h at a constant temperature of 21°C, allowed to settle down for 15 min and centrifuged for 5 min at 3500*g*. Thereafter, the remaining activity of ^{137}Cs in the liquid phase was determined and converted to milligrams of Cs per milliliter. The adsorbed amount of Cs in the solid phase (mg g^{-1}) was calculated from the difference between the concentration of Cs in the liquid phase before and after equilibrium. A linear function was used to describe the relation between the concentration of Cs in the liquid and solid phase as

$$C_s = K_d C_w \quad [15]$$

where K_d is the adsorption isotherm (mL g^{-1}), and C_w is the concentration of Cs in the liquid phase (mg cm^{-3}).

Modeling of Cesium Diffusion in Soil

To quantify the diffusion coefficient as a function of soil water and mucilage content, the measured profiles of Cs concentration were inversely simulated by solving a one-dimensional diffusion equation including a reactive term as

$$(\theta+\rho_b K_d)\frac{\partial C_w}{\partial t} = \frac{\partial}{\partial x}\left(\theta D \frac{\partial C_w}{\partial x}\right) - \mu(\theta+\rho_b K_d)C_w \quad [16]$$

where C_w is the concentration of Cs in the liquid phase (mg cm^{-3}), θ is the soil water content (cm^3 cm^{-3}), ρ_b is the bulk density of soil (g cm^{-3}), K_d is the partitioning factor describing the exchange of Cs between liquid and solid phase (cm^{-3} g^{-1} = mL g^{-1}), D is the diffusion coefficient (cm^2 s^{-1}), μ is the decay constant (s^{-1}), x is the space position along the soil (cm), and t is the time. Equation [16] was numerically solved in MATLAB using a finite difference method and its only unknown, D, was inversely adjusted to best reproduce the measured profiles of Cs concentration at different times. The inverse problem was solved by minimizing a predefined objective function (the difference between measured and simulated profiles of Cs) using the global optimization toolbox in MATLAB (pattern search algorithm).

Modeling of Nutrient Uptake by Plant Roots: A Simplified Scenario

Let us assume that effect of mucilage on the diffusion of K will be identical to the one of Cs. Then, in a simplified scenario, transport of K in soil and its uptake by a single plant root was numerically simulated by solving an advection–diffusion equation for the one-dimensional axisymmetric flow of water and nutrient toward the roots as

$$\frac{\partial(\theta+b)C_w}{\partial t} = \frac{\partial}{r\partial r}\left(\theta r D \frac{\partial C_w}{\partial r}\right) - \frac{\partial}{r\partial r}(r j_r C_w) \quad [17]$$

where b is the coefficient describing the adsorption of K by the solid phase (dimensionless), r is the radial distance from the root center (cm), j_r is the water flux in soil (cm s^{-1}), and the other variables were defined before. The right side of Eq. [17] includes the conservation of mass (concentration) between liquid and solid phases assuming an equilibrium. The coefficient b can be defined as

$$b = \rho_b K_d \quad [18]$$

and j_r can be calculated in two steps. In the first step, Richards' equation for one-dimensional axisymmetric flow is solved to get the profile of the matric potential as a function of distance from the root surface:

$$C(h)\frac{\partial h}{\partial t} = \frac{\partial}{r\partial r}\left[r k(h)\frac{\partial h}{\partial r}\right] \quad [19]$$

where $k(h)$ is the soil hydraulic conductivity as a function of soil matric potential and $C(h) = \partial h/\partial\theta$ (slope of soil water retention curve). Then j_r will be

$$j_r = k(h)\frac{\partial h}{\partial r} \quad [20]$$

Equation [17] and [20] were solved simultaneously in MATLAB using an implicit finite difference method for a one-dimensional soil domain with a distance of 1 cm from the root surface.

Parameterization of the Nutrient Uptake Model

To study the effect of mucilage on K uptake, Eq. [17] and [20] were solved for a soil domain consisting of two compartments; the rhizosphere (with a thickness of 0.125 mm from the root surface) and the bulk soil (from the edge of the rhizosphere with a thickness of 1 cm). Two contrasting scenarios were used to parametrize the hydraulic and diffusive properties of the soil domain: (i) both the rhizosphere and the bulk soil were parameterized based on the measured data of soil without mucilage; and (ii) in contrast with the first case, the hydraulic and diffusive properties of the rhizosphere domain were parameterized based on data of soil mixed with mucilage of chia seeds. For the latter case, it was assumed that the mucilage content (C_{tot}, mg dry mucilage g^{-1} dry soil) is zero at a distance of 0.125 cm from the root surface and increases linearly toward the root surface (Kroener et al., 2016). Note that based on this assumption, both hydraulic and diffusive properties of soil change as a function of distance from the root surface. The profile of mucilage content as a function of distance from the root surface is given in Supplemental Fig. S1.

The advection–diffusion equation was further parameterized based on the data of K uptake by maize plants reported by Seiffert et al. (1995). At the root surface (r_r), we presumed an uptake flux of Michaelis–Menten kinetics in the form of

$$j_s = \frac{K_m(C - C_{min})}{F_m + C - C_{min}} \quad [21]$$

where j_s is the K uptake rate (mg cm^{-2} s^{-1}), K_m is the maximum uptake rate of K per area of the soil–root interface (mg cm^{-2} s^{-1}), F_m is the Michaelis–Menten constant denoting the concentration at which the uptake of K is half of the possible uptake (mg cm^{-3}), C is the K concentration at the root surface (mg cm^{-3}), and C_{min} is the lowest concentration of K at which it can be taken up (mg cm^{-3}). These coefficients were taken from Seiffert et al. (1995) as follows: $K_m = 7.82 \times 10^{-4}$ mg cm^{-2} s^{-1}, $F_m = 3.21 \times 10^{-7}$ mg cm^{-3}, $C_{min} = 7.82 \times 10^{-5}$ mg cm^{-3}, and $C = 5.82 \times 10^{-2}$ mg cm^{-3} (for the scenario of a soil solution with a high K concentration) or $C = 5.82 \times 10^{-3}$ mg cm^{-3} (for the scenario of a soil solution with a low K concentration).

Equation [17] was used to simulate the profile of K concentration as a function of distance from the root surface during a soil drying cycle. Eight different scenarios were tested (Table 1), which vary in terms of mucilage presence, K concentration in the soil solution, and root water uptake rate. The parameterization of all scenarios was based on the data reported by Seiffert et al. (1995). In all cases, we assumed that the coefficient b describing the equilibrium between the concentration of K adsorbed to the solid and dissolved in the liquid phase was uniform across the rhizosphere and bulk soil and was equal to 8.61 as reported by Seiffert et al. (1995). With this assumption, the effect of mucilage on the adsorption of K was neglected, since this effect was beyond the scope of this study.

Results

The presence of mucilage at a content of 2.5 mg g^{-1} increased the volumetric water content of the soil at any given soil water potential (Fig. 2a). Equation [7] and [10] were successfully used to parameterize the relation between soil water potential and soil water content in soil with and without mucilage, respectively.

Table 1. Scenarios used to simulate profiles of K concentration as a function of distance from the root surface and its uptake by plant roots during soil drying. Scenarios vary in terms of mucilage presence, K concentration in the soil solution, and root water uptake rate.

Scenario†	Root water uptake rate	Initial concentration of K in the soil solution	Rhizosphere
	cm s^{-1}	mg cm^{-3}	
$K^LF^HR^-$	high: 1×10^{-5}	low: 5.82×10^{-3}	with mucilage
$K^LF^HR^+$	high: 1×10^{-5}	low: 5.82×10^{-3}	without mucilage
$K^LF^LR^-$	low: 2×10^{-6}	low: 5.82×10^{-3}	with mucilage
$K^LF^LR^+$	low: 2×10^{-6}	low: 5.82×10^{-3}	without mucilage
$K^HF^HR^-$	high: 1×10^{-5}	high: 5.82×10^{-2}	with mucilage
$K^HF^HR^+$	high: 1×10^{-5}	high: 5.82×10^{-2}	without mucilage
$K^HF^LR^-$	low: 2×10^{-6}	high: 5.82×10^{-2}	with mucilage
$K^HF^LR^+$	low: 2×10^{-6}	high: 5.82×10^{-2}	without mucilage

† R^+ and R^- refer to the scenarios of rhizosphere with and without mucilage, respectively; K^L and K^H refer to the scenarios of soil with a low and a high initial concentration of K, respectively; and F^L and F^H refer to the scenarios of a high and low root water uptake rate, respectively.

The saturated soil hydraulic conductivity was also affected by the presence of mucilage: with increasing mucilage contents, the saturated hydraulic conductivity was reduced (Fig. 2b), but as the soil dried, the presence of mucilage prevented the big drop in hydraulic

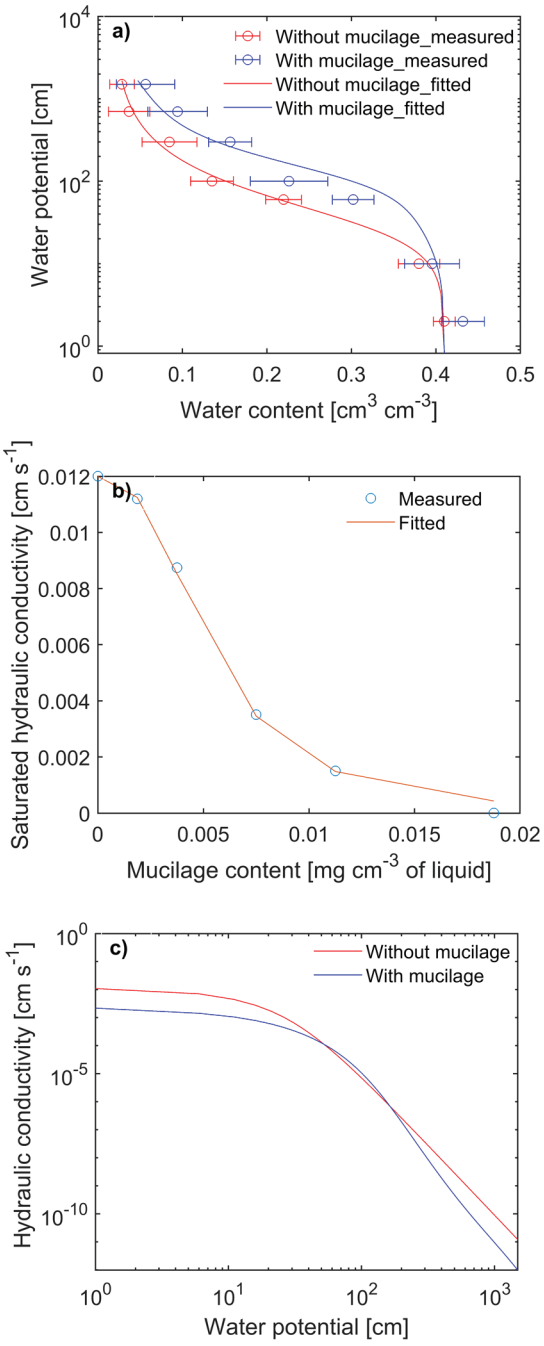

Fig. 2. (a) Measured and fitted water retention curves of soils with different mucilage contents (at a content of zero and 2.5 mg g^{-1}), with Eq. [7] and [10] fitted to the measured data (data are means of three replications and error bars indicate SDs); (b) measured and fitted saturated hydraulic conductivity of soil with different mucilage contents, with Eq. [13] fitted to these data to parameterize the effect of mucilage on viscosity of liquid phase (data are means of three replications and error bars indicate SDs); and (c) estimated hydraulic conductivity curve of soil with different mucilage contents (0 and 2.5 mg g^{-1}) based on parameterization of Eq. [12].

Table 2. Hydraulic properties of soil without mucilage. Parameters of the soil water retention curve were obtained from fitting Eq. [7] to the measured data. For parameterization of the soil hydraulic conductivity curve based on Eq. [11], saturated hydraulic conductivity (K_s) was measured and λ (a unitless factor describing the tortuosity of the diffusion path) was set to the one estimated in the diffusion experiment.

Equation	Coefficient†	Value
Eq. [7]	θ_r	0.017
	θ_s	0.41
	α, cm^{-1}	0.029
	n	1.92
Eq. [11]	K_s, $cm\ s^{-1}$	0.012
	λ	1.35

† θ_r, residual water content; θ_s, saturated water content; α and n are empirical coefficients.

Table 3. Hydraulic properties of soil mixed with mucilage at a content of 2.5 mg g^{-1}. Parameterization of the soil water retention curve was based on fitting Eq. [9] to the measured water retention curve. The soil hydraulic conductivity curve was parameterized by fitting Eq. [13] to the saturated hydraulic conductivity of soil as a function of different mucilage contents.

Equation	Coefficient†	Value
Eq. [9]	ω_1	8.49×10^5
	β_1	3.33
	ω_2	2.29×10^3
	β_2	8.65×10^{-1}
Eq. [13]	C_0	5.29×10^{-3}
	C_1	2.59
	d_0	2.94
	d_1	65.30

† ω_1, β_1, ω_2, and β_2 are fitting parameters; C_0, C_1, d_0, and d_1 are fitting parameters that were determined by fitting Eq. [12] to the measured data of saturated hydraulic conductivities of soil at different mucilage contents.

conductivity of soil (Fig. 2c). Equation [12] was fitted to the data of saturated hydraulic conductivity to estimate its parameters, which were needed to parameterize the hydraulic conductivity curve of soil treated with mucilage. The hydraulic properties of soils with and without mucilage are given in Tables 2 and 3. These tables show the parameterization of soil water retention curve and soil hydraulic conductivity of control soil and soil mixed with mucilage. Diffusion-driven transport of Cs in soils with and without mucilage are shown in Fig. 3. This exemplary result shows a color map proportional to the Cs concentration in the soil (i.e., red and blue parts indicate regions of high and low activities, respectively). With time, Cs diffused from the left side of the containers to their right side. This diffusive transport was affected by the soil water content and was slower at low water contents. Comparing soil with and without mucilage at a water content of 0.20 and 0.13 $cm^3\ cm^{-3}$ showed that the presence of mucilage maintained slightly higher diffusive transport rates. The ^{137}Cs activity was further quantified through image processing and using the calibration function presented in Supplemental Fig. S2.

Figure 4 shows the profile of the Cs concentration as a function of position within the soil samples at different times for soils mixed with and without mucilage at water contents of 0.30 and 0.13 $cm^3\ cm^{-3}$. At a water content of 0.30 $cm^3\ cm^{-3}$, the Cs concentration profiles were similar in both soils with and without mucilage, and Cs was more uniformly distributed across the soil after 159 h (Fig. 4a and 4b). At the soil water content of 0.13 $cm^3\ cm^{-3}$, diffusion was significantly reduced in both soils but the reduction was lower in the soil treated with mucilage (Fig. 4c and 4d). Presence of mucilage prevented a marked drop in the diffusion of Cs as the soil dried.

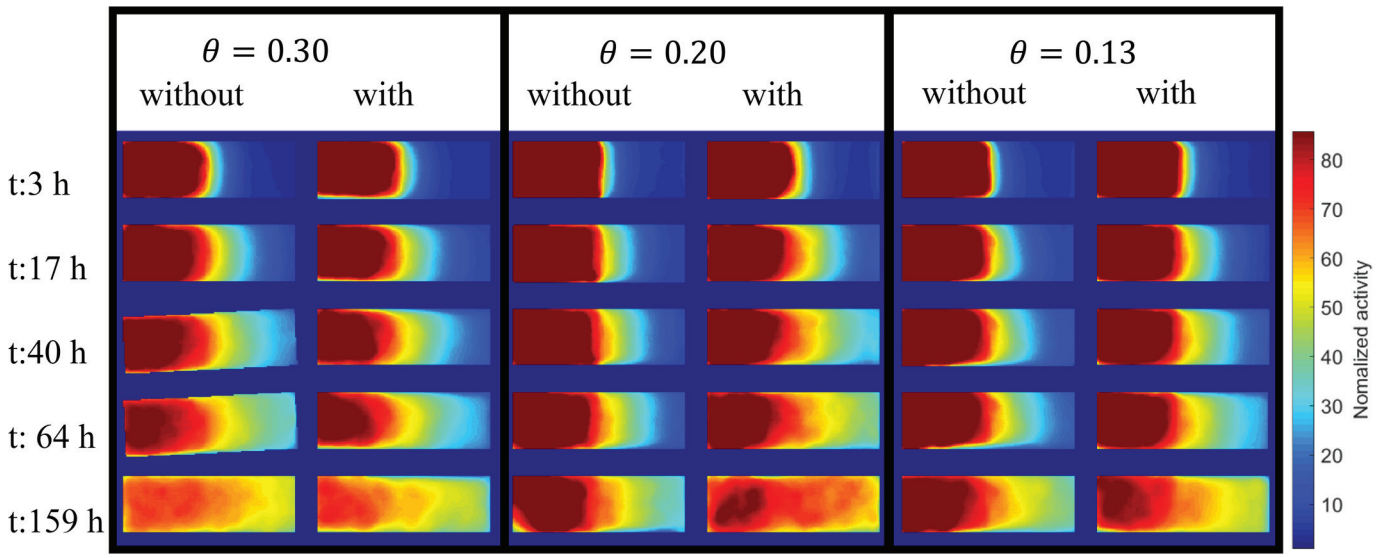

Fig. 3. Example images of ^{137}Cs distribution in soils treated with mucilage and controls at varying times (t) and varying soil water contents (θ). The color map shows the normalized activity of ^{137}Cs (i.e., red color indicates high activity of ^{137}Cs and blue low or zero activity).

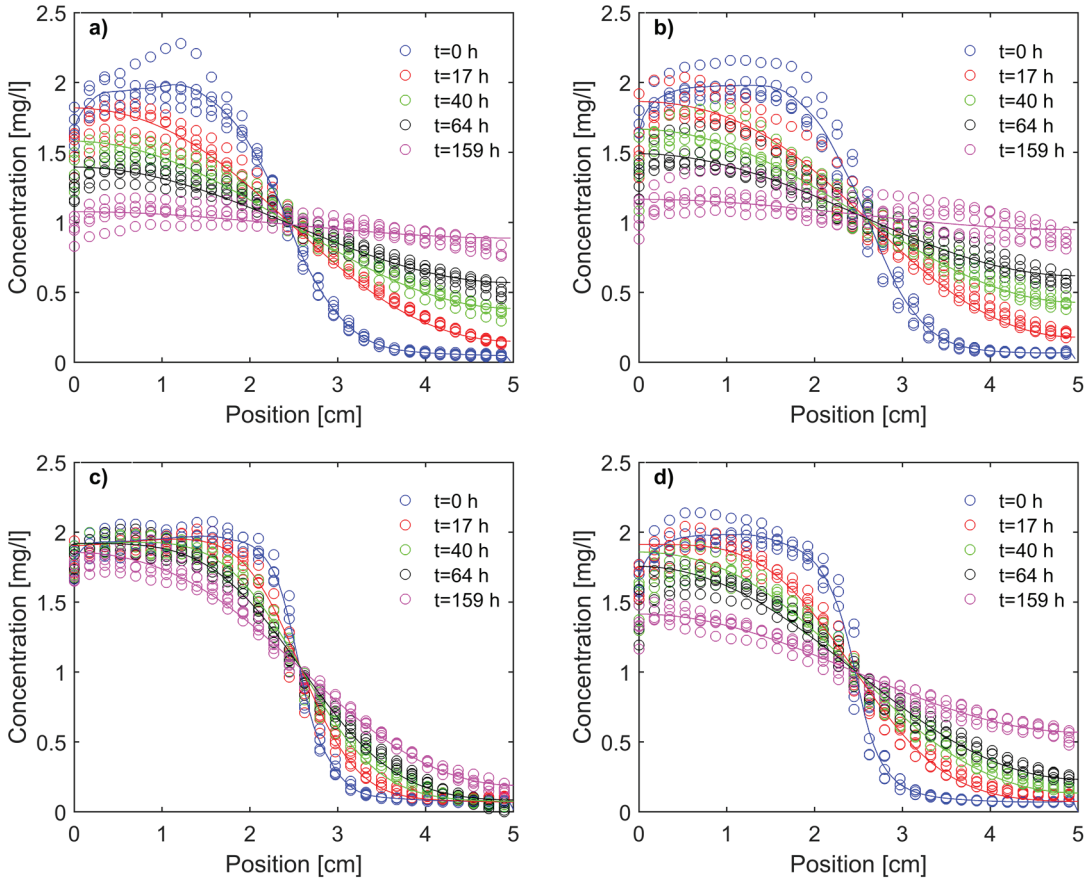

Fig. 4. Example profiles of the Cs concentration at different times (t): (a) soil without mucilage at a water content of 0.30 cm^3 cm^{-3}; (b) soil with mucilage at a water content of 0.30 cm^3 cm^{-3}; (c) soil without mucilage at a water content of 0.13 cm^3 cm^{-3}; and (d) soil with mucilage at a water content of 0.13 cm^3 cm^{-3}. The dots refer to the data of phosphor imaging of five replications, and lines are the fitted concentration profiles according to Eq. [16]. Here, position refers to the length of the soil containers starting from the left side.

In addition to the diffusion coefficient, the exchange of Cs between the solid and liquid phase of soil was also affected by the presence of mucilage (shown in Supplemental Fig. S3). The relationship between the Cs concentrations in the liquid and solid phase in the expected range was well described by a linear function with a constant rate (slope) of $K_d = 4.41 \times 10^{-5}$ cm^3 mg^{-1} for soils without mucilage and $K_d = 2.10 \times 10^{-5}$ cm^3 mg^{-1} for soils with mucilage.

With a known K_d, Eq. [16] was inversely fitted to the profiles of Cs concentration by adjusting the diffusion coefficients (Fig. 4). The diffusion coefficient of Cs was strongly affected by soil water content and decreased as the soil dried (Fig. 5). The presence of mucilage attenuated the change of the diffusion coefficient of soil as it dries. When the soil was wet, the diffusion coefficient was similar in treated and untreated soils. Under dry conditions (soil water content of 0.13 cm^3 cm^{-3}), mucilage led to an increase in the diffusion coefficient of soil by 3.35 times compared with its control without mucilage. The relationship between the diffusion coefficient and the soil water content was well described by Eq. [3] for both treated and untreated soils (Fig. 5).

In a series of simple scenarios (Table 1), the effect of mucilage on the transport and uptake of K by a single root during soil

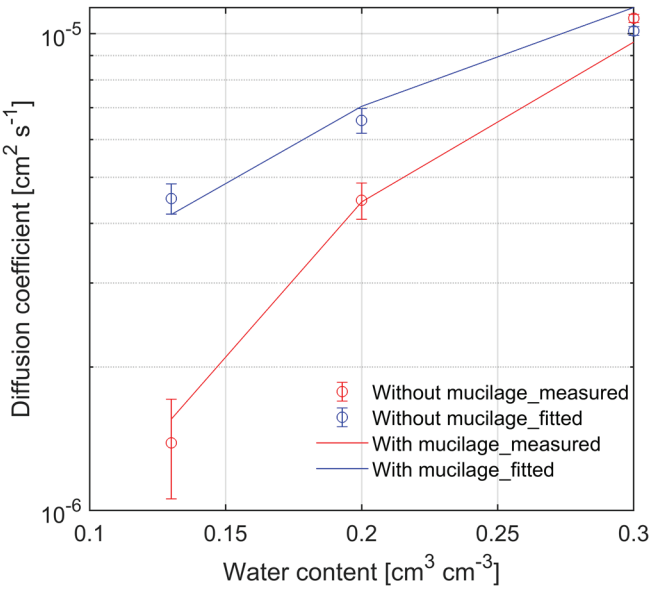

Fig. 5. Measured and fitted diffusion coefficients of Cs in untreated and mucilage-treated soil at varying soil water contents. The data are means of five replications and the error bars indicate the SDs. The lines show fitted profiles of the diffusion coefficient as a function of soil water content according to Eq. [3]. It can be seen that mucilage prevented a big drop in diffusion coefficient of Cs as soil dries.

drying soil was investigated (Eq. [17]). Figure 6 shows the profiles of K as a function of the distance from the root surface (the first 1.6 mm are shown) for eight different scenarios at varying times during a soil drying cycle. In the case of low concentration of K (Fig. 6a and 6c), a depletion zone appeared near the root surface under both high and low root water uptake rates. Mucilage prevented a big drop in concentration in the vicinity of the root by extending the depletion zone toward the bulk soil. In both cases, the concentration of K initially decreased as the soil dried and K was taken up by the plant root. With further soil drying (decreasing soil water content), the gradient at the root surface became steeper while the concentration of K in the bulk soil increased. Note that K content stayed constant while the water content decreased, resulting in a higher concentration. In the case of high K concentration in the soil solution (Fig. 6b), when root water uptake was assumed to be high, the concentration of K at the root surface increased as the soil dried and a steep gradient in K concentration developed in the immediate vicinity of the root. The presence of mucilage prevented the development of such a big gradient. In summary, these results show that mucilage maintains the diffusive transport of K under drying condition and prevents steep gradients at the root surface (depletion and accumulation).

To better illustrate the effect of mucilage on the concentration of K near the root and its uptake by the plant, the concentration of K at the root surface and its simulated uptake is shown in Fig. 7. In this figure, the total nutrient uptake is calculated assuming a root length of 1 cm and a root radius of 0.0195 cm as reported by Seiffert et al. (1995). In the case of high root water uptake rate and high K concentration in the soil solution (Fig. 7a, scenario $K^{H}F^{H}R^{-}$), the K concentration tended to increase at the root surface, particularly as the soil dried and the contribution of mass flow became dominant. Mucilage in the rhizosphere, in this case (Fig. 7a, scenario $K^{H}F^{H}R^{+}$), delayed the accumulation of K at the root surface. In the case of high root water uptake, when the K concentration was low in the soil solution (Fig. 7a, scenario $K^{L}F^{H}R^{-}$), a depletion zone in the vicinity of the root developed as the soil dried. Again, mucilage prevented the marked drop in K concentration at the root surface by maintaining a high diffusion of K (Fig. 7a, scenario $K^{L}F^{H}R^{+}$). As a consequence, total K uptake by the plant was higher in the case of soil with mucilage than in its control (Fig. 7b and 7d). When the root water uptake rate was assumed to be lower (decreased by a factor of five times, Fig. 7c), a depletion zone in the vicinity of the root was developed as the soil dried. This depletion was observed in both cases of soil solution with high and low concentrations of K, but the presence

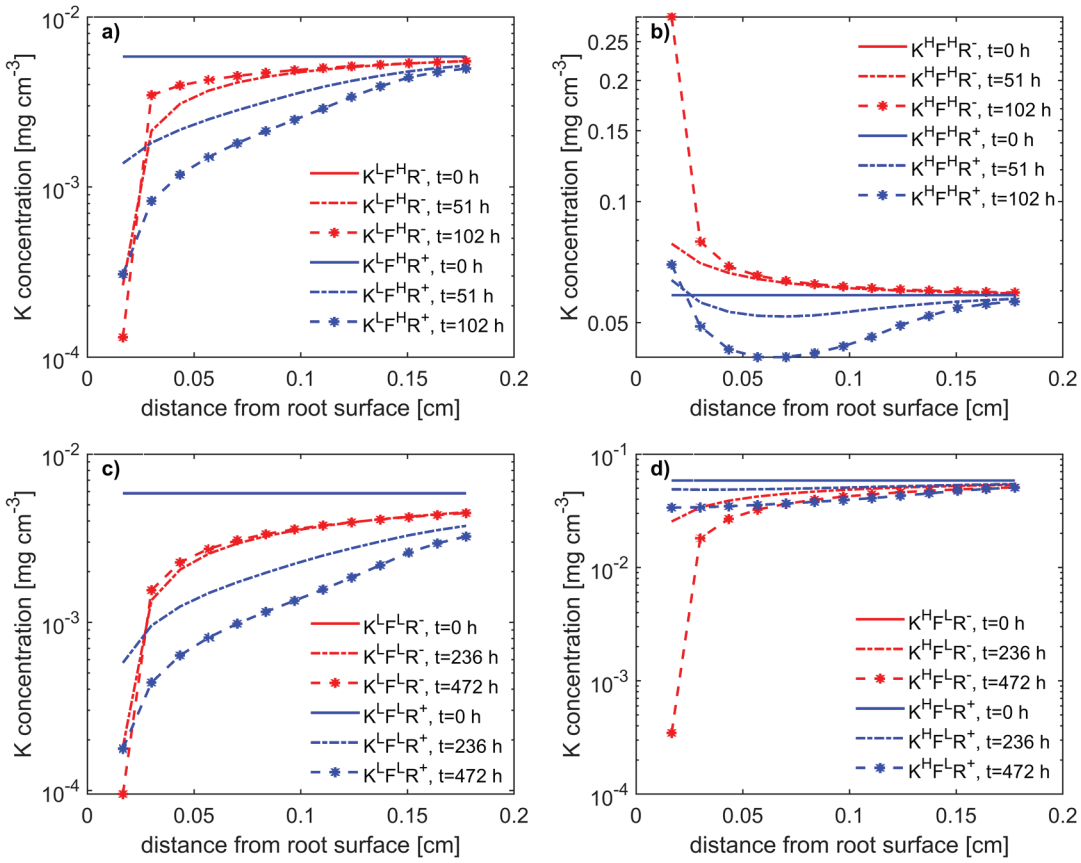

Fig. 6. Simulated profiles of K concentration as a function of distance from the root surface during soil drying and times during a soil drying cycle (t). The solid lines refer to soil with mucilage, and the dashed lines to the soil without mucilage. R^{+} and R^{-} refer to the scenarios of rhizosphere with and without mucilage, respectively; K^{L} and K^{H} refer to the scenarios of soil with a low and a high initial concentration of K, respectively; and F^{L} and F^{H} refer to the scenarios of a high and low root water uptake rate, respectively. The scenarios and the legend of figures are described in detail in Table 1.

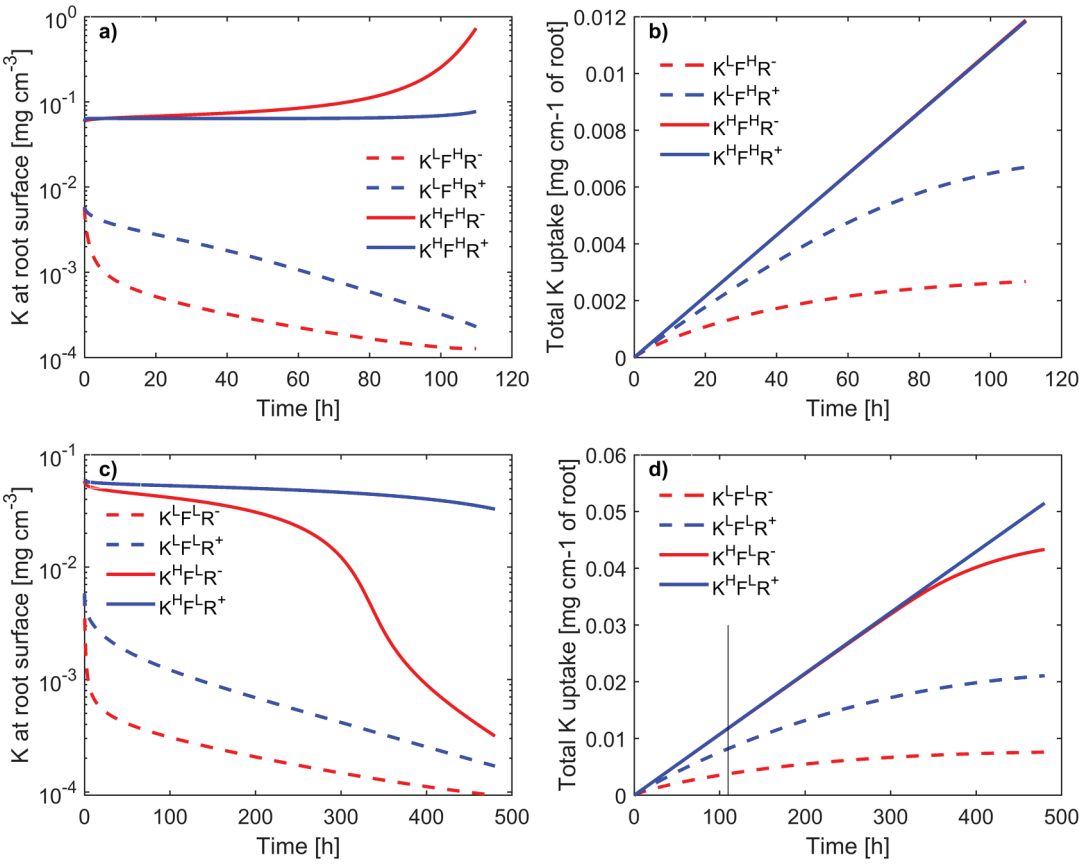

Fig. 7. (a,c) Simulated K concentration at the root surface and (b,d) its uptake by plants considering different scenarios. R^+ and R^- refer to the scenarios of rhizosphere with and without mucilage, respectively; K^L and K^H refer to the scenarios of soil with a low and a high initial concentration of K in the soil solution, respectively; and F^L and F^H refer to the scenarios of high and low root water uptake rate, respectively. The tested scenarios and the legend of figures are described in detail in Table 1. The back line in Fig. 7d shows the time at which soil was dried in scenarios with high root water uptake rate.

of mucilage in the rhizosphere moderates its development, which resulted in a higher K uptake.

Discussion

Soil drying restricts the diffusion of K. As soil dries, the cross-sectional area of the liquid phase available for diffusion decreases while the tortuosity of the flow path increases. Both processes limit diffusion. At a mucilage content of 2.5 mg g^{-1}, a marked drop in the diffusion rate of K is prevented. This allowed for a higher diffusion rate of K across a wider range of soil water contents (Fig. 5).

The effect of mucilage on nutrient diffusion can be explained by two main processes: (i) when soil dries, mucilage keeps the rhizosphere wet due to its high water-holding capacity (McCully and Boyer, 1997; Carminati et al., 2010) and therefore maintains the diffusive transport of nutrients at a higher rate, and (ii) mucilage alters the spatial configuration of the liquid phase and increases its connectivity in drying soil due to its unique properties (water sorption, high viscosity, and low surface tension) (Carminati et al., 2017; Benard et al., 2018). The latter one was the focus of the experiments performed herein to monitor the diffusion coefficient of Cs. The diffusion coefficient of Cs was determined at different mucilage contents (zero and 2.5 mg g^{-1}) and varying soil water contents. For the same water content, it was found that under dry conditions ($\theta = 0.13$ cm^3 cm^{-3}), the diffusion coefficient was 3.35 times higher in the model rhizosphere soil than in its control. Since the soil water content was equal, the difference in diffusion coefficient can be safely assigned to change in spatial distribution of liquid phase within the soil pore spaces. The increase in viscosity of the liquid phase due to the presence of mucilage as the soil dries allows water (liquid phase) to stay connected and aid the diffusion of Cs through a continuous film within the pore space (Carminati et al., 2017; Benard et al., 2018).

The soil-drying scenarios (Table 1) showed that the presence of mucilage in the rhizosphere altered the spatial distribution of K in the soil and consequently may improve the K uptake by plant roots in drying soil (Fig. 7). Considering a soil with low K concentration in the soil solution and rhizosphere soil without mucilage, a drastic depletion of K concentration developed around the roots as the soil dries and the plant takes up nutrients (Fig. 6). Mucilage attenuated such steep concentration gradients near the roots and sustained a higher K uptake by extending the depletion zone toward the bulk soil. Our findings suggest that mucilage may favor uptake of nutrients with low concentration in the soil solution of drying soil (e.g., microelements) by delaying their depletion at the root surface. Considering a soil with mucilage-free rhizosphere

and high K concentration in the soil solution, K appeared to be accumulated at the root surface as soil dried by high root water uptake rates. In this case, when soil dried, the K diffusion rate decreased and therefore the contribution of convective transport became dominant, resulting in the accumulation of K at the root surface, as predicted by similar models (de Jong van Lier et al., 2009; Schröder et al., 2014). For the case of mucilage in the rhizosphere, the accumulation of K was substantially delayed, reducing the risk of salinity stress as soil dries.

In this study, the effect of mucilage on K transport and uptake was investigated by modeling nutrient transport toward a single root under the assumption of steady-state root water uptake. Our findings highlight the potential effects of mucilage on nutrient uptake by alteration of the physical properties of the soil solution. These complex aspects of mucilage on nutrient uptake are not yet considered in recent models of root water and nutrient uptake. Other processes not included in the presented model might also be linked to these physical alterations of the rhizosphere. For instance, it has been shown that mucilage affects the equilibrium between soil water content and soil water potential in the rhizosphere, which results in less fluctuation of water content in the rhizosphere (Kroener et al., 2014; Schwartz et al., 2016). Secondly, the concentration of nutrients or salts at the root surface (particularly their accumulation during soil drying) may result in reduced root water uptake (de Jong van Lier et al., 2009; Schröder et al., 2014).

The findings of this study were based on experiments with mucilage extracted from chia seeds mixed with a sandy soil at a content of 2.5 mg g^{-1} soil. Ideally, the measurements should be performed with plant root mucilage. It has recently been shown that the physical properties of mucilage (water sorption, surface tension, and viscosity) differs among plant seedlings and chia seeds (Naveed et al., 2019). Besides being plant specific, the physical properties may additionally vary depending on the plant growth condition, soil texture, and mechanical stress. These variations do not allow for the selection of one representative mucilage. Considering their impact on the physical properties of the liquid phase, all mucilages (plant root and seed mucilages) show similar intrinsic properties; they reduce the surface tension, increase the viscosity of liquid phase, and increase water sorption. These are the key properties to enhance liquid connectivity in drying soil and to maintain the diffusive transport of nutrients (Benard et al., 2019). Naveed et al. (2019) showed that chia seed mucilage has the highest viscosity, followed by mucilage of maize and barely seedling. For this reason, it is probable that higher contents of maize and barely mucilage would be needed to observe a similar effect as reported in this study. Considering the soil type, we used washed sandy soil with no organic matter. If we only consider the diffusion of nutrients in soil, excluding the effect of soil type on adsorption of nutrients, we may expect similar effects of mucilage on diffusion coefficients but at a different mucilage content. It is shown that in a fine-textured soil, less mucilage content is needed to affect the water-holding capacity of the soil (Kroener et al., 2018). It should be also mentioned that the method used here based on tracing ^{137}Cs transport may not be applicable in the case of fine-textured soil (with clay particle). In such a case, ^{137}Cs will be strongly adsorbed onto the clay particles and its transport will be slowed down dramatically.

In conclusion, mucilage can favor the transport of nutrients in drying soil and their uptake by plant roots. The main drivers are the mucilage-induced increase in soil moisture and the enhanced connectivity of the liquid phase in the rhizosphere. At the plant scale, mucilage may reduce the risk of nutrient deficiencies and salinity stress and therefore increase drought tolerance.

Supplemental Material

Supplemental Fig. S1 depicts profiles of mucilage content and volumetric soil water content as a function of distance from the root surface. Supplemental Fig. S2 depicts the calibration lines used to relate the normalized color intensity in the phosphor imaging to the activity of the Cs. Supplemental Fig. S3 depicts the Cs adsorption behavior of the soil with and without mucilage.

Acknowledgments

We would like to thank Bernd Kopka from the Laboratory for Radioisotopes (LARI) of the University of Goettingen for their advice, support, and measurements. We also thank Andrea Carminati, Yakov Kuzyakov, and Norbert Claassen for their helpful advice and discussions on the various aspects of this work. We also thank the associated editor, Jean Caron, and two anonymous reviewers for helpful and constructive suggestions and comments on the previous version of the manuscript. Their comments and suggestions improved the consistency and generality of this manuscript. This publication was funded by the German Research Foundation (DFG) and the University of Bayreuth in the funding program Open Access Publishing.

References

Banfield, C.C., M. Zarebanadkouki, B. Kopka, and Y. Kuzyakov. 2017. Labelling plants in the Chernobyl way: A new ^{137}Cs and ^{14}C foliar application approach to investigate rhizodeposition and biopore reuse. Plant Soil 417:301–315. doi:10.1007/s11104-017-3260-7

Benard, P., M. Zarebanadkouk, M. Brax, R. Kaltenbach, I. Jerjen, F. Marone, et al. 2019. Microhydrological niches in soils: How mucilage and EPS alter the biophysical properties of the rhizosphere and other biological hotspots. Vadose Zone J. 18:180211. doi:10.2136/vzj2018.12.0211

Benard, P., M. Zarebanadkouki, and A. Carminati. 2018. Physics and hydraulics of the rhizosphere network. J. Plant Nutr. Soil Sci. 182:5–8. doi:10.1002/jpln.201800042

Benard, P., M. Zarebanadkouki, C. Hedwig, M. Holz, M.A. Ahmed, and A. Carminati. 2017. Pore-scale distribution of mucilage affecting water repellency in the rhizosphere. Vadose Zone J. 17:170013. doi:10.2136/vzj2017.01.0013

Carminati, A., P. Benard, M.A. Ahmed, and M. Zarebanadkouki. 2017. Liquid bridges at the root-soil interface. Plant Soil 417:1–15. doi:10.1007/s11104-017-3227-8

Carminati, A., A.B. Moradi, D. Vetterlein, P. Vontobel, E. Lehmann, U. Weller, et al. 2010. Dynamics of soil water content in the rhizosphere. Plant Soil 332:163–176. doi:10.1007/s11104-010-0283-8

Carminati, A., and D. Vetterlein. 2013. Plasticity of rhizosphere hydraulic properties as a key for efficient utilization of scarce resources. Ann. Bot. 112:277–290. doi:10.1093/aob/mcs262

Chou, H., L. Wu, L. Zeng, and A. Chang. 2012. Evaluation of solute diffusion tortuosity factor models for variously saturated soils. Water Resour. Res. 48:W10539. doi:10.1029/2011WR011653

Darrah, P.R. 1993. The rhizosphere and plant nutrition: A quantitative approach. Plant Soil 155–156:1–20. doi:10.1007/BF00024980

Hinsinger, P., A.G. Bengough, D. Vetterlein, and I.M. Young. 2009. Rhizosphere: Biophysics, biogeochemistry and ecological relevance. Plant Soil 321:117–152. doi:10.1007/s11104-008-9885-9

Holz, M., M. Zarebanadkouki, A. Kaestner, Y. Kuzyakov, and A. Carminati. 2018. Rhizodeposition under drought is controlled by root growth rate and rhizosphere water content. Plant Soil 423:429–442. doi:10.1007/s11104-017-3522-4

Jones, D.L., C. Nguyen, and R.D. Finlay. 2009. Carbon flow in the rhizosphere: Carbon trading at the soil-root interface. Plant Soil 321:5–33. doi:10.1007/s11104-009-9925-0

de Jong van Lier, Q., J.C. van Dam, and K. Metselaar. 2009. Root water extraction under combined water and osmotic stress. Soil Sci. Soc. Am. J. 73:862–875. doi:10.2136/sssaj2008.0157

Kroener, E., M. Holz, M. Zarebanadkouki, M. Ahmed, and A. Carminati. 2018. Effects of mucilage on rhizosphere hydraulic functions depend on soil particle size. Vadose Zone J. 17:170056. doi:10.2136/vzj2017.03.0056

Kroener, E., M. Zarebanadkouki, M. Bittelli, and A. Carminati. 2016. Simulation of root water uptake under consideration of nonequilibrium dynamics in the rhizosphere. Water Resour. Res. 52:5755–5770. doi:10.1002/2015WR018579

Kroener, E., M. Zarebanadkouki, A. Kaestner, and A. Carminati. 2014. Nonequilibrium water dynamics in the rhizosphere: How mucilage affects water flow in soils. Water Resour. Res. 50:6479–6495. doi:10.1002/2013WR014756

Kuzyakov, Y. 2010. Priming effects: Interactions between living and dead organic matter. Soil Biol. Biochem. 42:1363–1371. doi:10.1016/j.soilbio.2010.04.003

Lim, P.C., S.L. Barbour, and D.G. Fredlund. 1998. Influence of degree of saturation on the coefficient of aqueous diffusion. Can. Geotech. J. 35:811–827. doi:10.1139/t98-045

McCully, M.E., and J.S. Boyer. 1997. The expansion of maize root-cap mucilage during hydration: 3. Changes in water potential and water content. Physiol. Plant. 99:169–177. doi:10.1111/j.1399-3054.1997.tb03445.x

Moldrup, P., T. Olesen, T. Komatsu, P. Schjønning, and D.E. Rolston. 2001. Tortuosity, diffusivity, and permeability in the soil liquid and gaseous phases. Soil Sci. Soc. Am. J. 65:613–623. doi:10.2136/sssaj2001.653613x

Moyano, F.E., S. Manzoni, and C. Chenu. 2013. Responses of soil heterotrophic respiration to moisture availability: An exploration of processes and models. Soil Biol. Biochem. 59:72–85. doi:10.1016/j.soilbio.2013.01.002

Naveed, M., M.A. Ahmed, P. Benard, L.K. Brown, T.S. George, A.G. Bengough, et al. 2019. Surface tension, rheology and hydrophobicity of rhizodeposits and seed mucilage influence soil water retention and hysteresis. Plant Soil 437:65–81. doi:10.1007/s11104-019-03939-9

Naveed, M., L.K. Brown, A.C. Raffan, T.S. George, A.G. Bengough, T. Roose, et al. 2017. Plant exudates may stabilize or weaken soil depending on species, origin and time. Eur. J. Soil Sci. 68:806–816. doi:10.1111/ejss.12487

Oades, J.M. 1978. Mucilage at the root surface. J. Soil Sci. 29:1–16. doi:10.1111/j.1365-2389.1978.tb02025.x

Oburger, E., and D.L. Jones. 2018. Sampling root exudates: Mission impossible? Rhizosphere 6:116–133. doi:10.1016/j.rhisph.2018.06.004

Read, D.B., and P.J. Gregory. 1997. Surface tension and viscosity of axenic maize and lupin root mucilages. New Phytol. 137:623–628. doi:10.1046/j.1469-8137.1997.00859.x

Read, D.B., P.J. Gregory, and A.E. Bell. 1999. Physical properties of axenic maize root mucilage. Plant Soil 211:87–91. doi:10.1023/A:1004403812307

Schröder, N., N. Lazarovitch, J. Vanderborght, H. Vereecken, and M. Javaux. 2014. Linking transpiration reduction to rhizosphere salinity using a 3D coupled soil-plant model. Plant Soil 377:277–293. doi:10.1007/s11104-013-1990-8

Schwartz, N., A. Carminati, and M. Javaux. 2016. The impact of mucilage on root water uptake: A numerical study. Water Resour. Res. 52:264–277. doi:10.1002/2015WR018150

Seiffert, S., J. Kaselowsky, A. Jungk, and N. Claassen. 1995. Observed and calculated potassium uptake by maize as affected by soil water content and bulk density. Agron. J. 87:1070–1077. doi:10.2134/agronj1995.00021962008700060007x

The MathWorks. 2017. MATLAB. Version 9.3.0 (R2017b). The MathWorks, Natick, MA.

Walker, T.S. 2003. Root exudation and rhizosphere biology. Plant Physiol. 132:44–51. doi:10.1104/pp.102.019661

Walker, T.S., H.P. Bais, E. Grotewold, and J.M. Vivanco. 2003. Root exudation and rhizosphere biology. Plant Physiol. 132:44–51. doi:10.1104/pp.102.019661